INJURY BIOMECHANICS RESEARCH
Proceedings of the Forty-Seventh International Workshop

Comparison of the THOR-50M IR-TRACC Measurement Device to an Alternative S-Track Measurement Device

A.V. Hagedorn[1], M.M. Murach[1], W.M. Millis[2], J. McFadden[2], D. Parent[3]
[1] Transportation Research Center Inc., East Liberty, OH, USA
[2]National Highway Traffic Safety Administration, VRTC, East Liberty, OH, USA
[3]National Highway Traffic Safety Administration, Washington, DC, USA

ABSTRACT

The THOR-50M drawing package specifies six Infrared Telescoping Rods for Assessment of Chest Compression (IR-TRACC) measurement devices: four in the thorax and two in the abdomen. In both NHTSA-sponsored testing and industry experience, these IR-TRACC devices have presented various issues. The objective of this study is to identify and evaluate a commercially-available alternative to the IR-TRACC 3-dimensional deflection measuring device for THOR-50M. The S-Track, which uses a scissor mechanism to achieve a linear deflection measurement, was identified and purchased. The size and weight of the S-Track allows direct replacement of the IR-TRACC in the double-gimbaled IR-TRACC assemblies found in the upper thorax, lower thorax, and abdomen of the THOR-50M. The evaluation strategy includes 1.) installation tests in an ATD to validate the integration, 2.) a series of calibration tests to validate the sensor's properties, 3.) quasi-static tests to validate the sensor's accuracy, and 4.) dynamic impact tests to the THOR-50M to verify the sensor's performance in thorax and abdomen qualification tests and sled tests. Tests were conducted with both the IR-TRACC and the S-Track in order to compare performance and output. Preliminary results suggest that S-Track is functionally equivalent to the IR-TRACC within the expected test-to-test variability. This study also proposes a framework to evaluate the equivalence of ATD design modifications at three levels of increasing complexity: component, ATD, and system.

INTRODUCTION

The current drawing package for the THOR-50M Anthropomorphic Test Device (ATD) specifies six Infrared Telescoping Rods for Assessment of Chest Compression (IR-TRACC) measurement devices: four in the thorax and two in the abdomen (NHTSA drawing package, 2018). These devices measure the absolute point-to-point distance along their length, which is used in the calculation of thorax and abdomen compression. When coupled with two rotational potentiometers to form a double-gimbal arrangement, the three-dimensional position of the anterior attachment points can be calculated.

NHTSA is generally satisfied by the performance of the IR-TRACC. However, it is an expensive instrument susceptible to damage in overload tests, and is only available from a single source. Also, during NHTSA-sponsored testing, noise has been observed in the recorded IR-TRACC data channels that is believed to be non-physical because it occurs in all IR-TRACC voltage channels at the same points in time (Figure 1) (Saunders, et. al., 2018). Figure 2 shows the position data calculated from the IR-TRACC output voltage. These examples are from a THOR-50M (SN 16) in the driver's seat during a left oblique 15°/35% offset crash test of a 2015 Honda Fit (R20155373). The noise was originally observed by Rouhana et al. (1998), who noted that it could adversely affect injury risk computations using the V*C algorithm in which the velocity is computed by digital differentiation of the IR-TRACC signal.

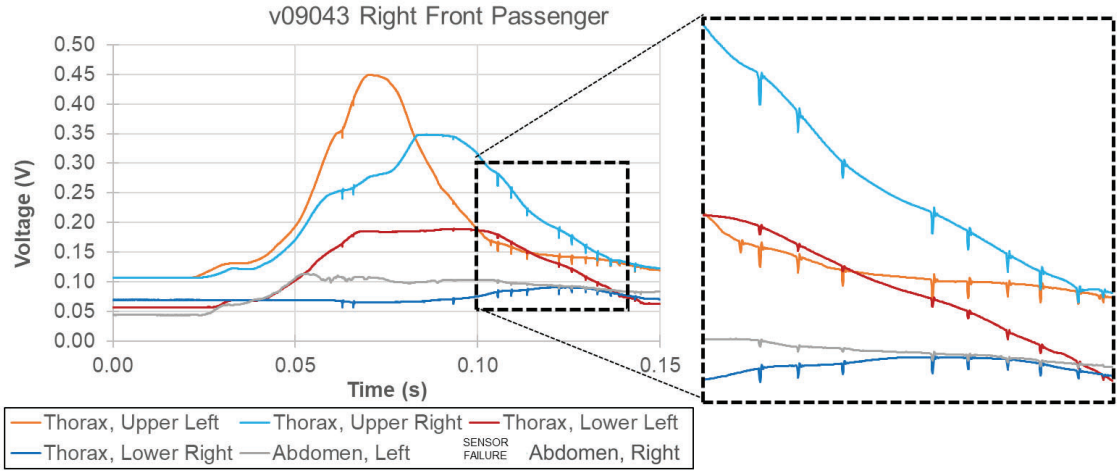

Figure 1: Example of noise seen in IR-TRACC voltage during NHTSA crash testing

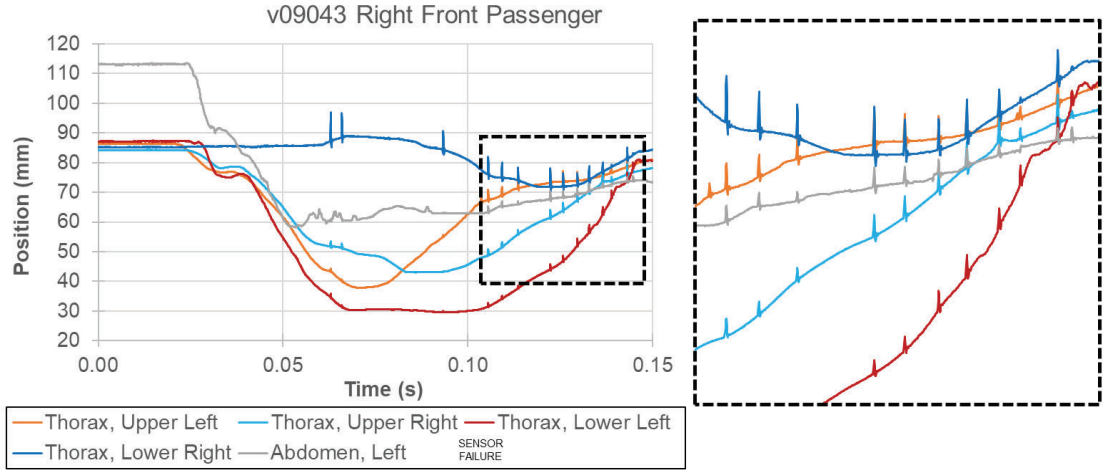

Figure 2: Example of noise seen in IR-TRACC position during NHTSA crash testing

The goal of this project was to review and evaluate one alternative to the IR-TRACC deflection measuring device for the THOR-50M. The S-Track (Figure 3) is a measurement device manufactured by ATD LabTech that implements a scissor mechanism to achieve a linear deflection measurement. The size and weight of the S-Track is intended to directly replace the IR-TRACC in the double-gimbaled IR-TRACC assemblies found in the upper thorax, lower thorax, and abdomen of the THOR-50M. Both static and dynamic evaluations of the S-Track were performed and compared to the IR-TRACC in order to determine if the S-Track is functionally equivalent to an IR-TRACC.

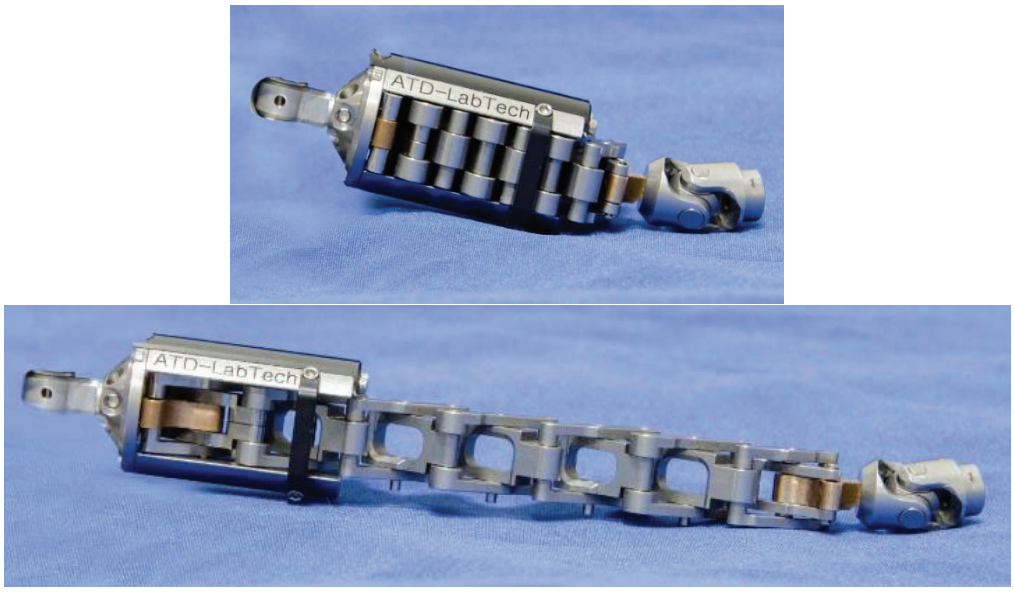

Figure 3: S-Track measurement device

METHODS

Evaluation Process

This paper describes one example of the evaluation process that was carried out to confirm the equivalence of alternate component designs to those defined in the THOR-50M drawing package. More generally, the evaluation process should evaluate equivalence at three levels: component, ATD, and system. There are many similarities in the three evaluations carried out, but the details differ based on the specific component being evaluated.

The component-level evaluation should verify that the alternate and baseline designs have the same functional properties in isolation. This could mean the same physical response, such as the moment-rotation characteristic of an alternate shoulder design, or the same function, such as the measurement range and accuracy of the alternate thorax and abdomen instrumentation.

The ATD-level evaluation should verify that an ATD with the alternate design installed meets the same qualification specifications as the baseline design. This could involve running one, many, or all qualification tests on the alternate design based on the scope of the alternate design.

The system-level evaluation is the most subjective of the evaluation levels, as it depends on the implementation of the ATD. In theory, the response of the alternate configuration of the ATD must be within the range of test-to-test variation of the baseline ATD. This would ensure that the alternate ATD configuration would result in the same test outcome as the baseline ATD configuration. For example, in a research test evaluating advanced restraint systems, the alternate and baseline ATD configurations would be expected to demonstrate equivalent injury risk. The degree to which this equivalence must be demonstrated, however, depends on the risk tolerance of the user.

Evaluation Approach

Both static and dynamic tests were conducted to compare the IR-TRACC and S-Track devices. Static tests included: 1.) installation in the THOR-50M to validate fit, 2.) calibration tests to validate the sensor's properties, and 3.) static positioning tests to validate the sensor's accuracy. Dynamic tests to validate the sensor's performance and durability included: 1.) qualification tests, and 2.) sled tests. Tests were conducted with both the IR-TRACC and the S-Track in order to compare performance and output. Both S-Tracks and IR-TRACCs were installed into the double-gimbal assembly obtained from a THOR-50M (Figure 4 and Figure 5).

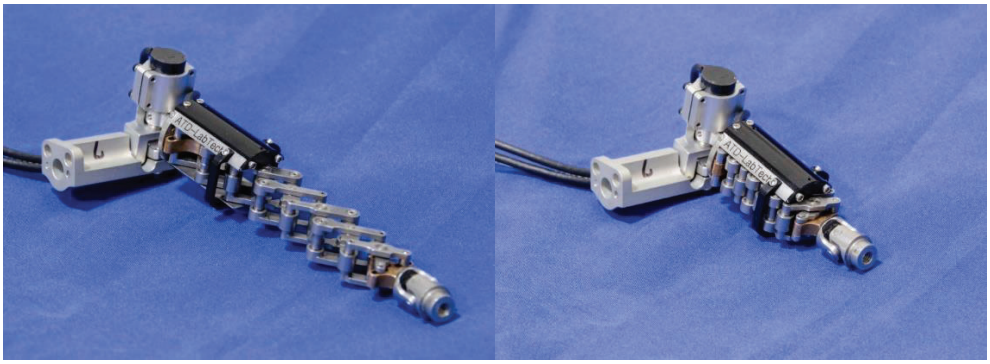

Figure 4: S-Track installed in double gimbal assembly

Figure 5: IR-TRACC installed in double gimbal assembly

Static Tests

Static tests included installation, calibration tests, and static positioning tests.

Installation. Each sensor was evaluated for equivalency of size and range of measurement. Both IR-TRACC and S-Track units were then installed into the thorax and abdomen locations in the THOR-50M to validate the fit of each device. Table 1 shows a comparison between the IR-TRACC and S-Track mass and diameter. The S-Track has a slightly higher mass and diameter compared to the IR-TRACC, but still fits into the same space as the IR-TRACC without issue.

Table 1. Mass and Diameter Comparison Between IR-TRACC and S-Track

	IR-TRACC Mass (kg)	S-Track Mass (kg)	IR-TRACC Max Dia. (mm)	S-Track Max Dia. (mm)
Upper & Lower Thorax	0.125	0.127	29.0	32.5
Lower Abdomen	0.159	0.152	31.6	32.6

Calibration Tests. The sensors were calibrated to ensure proper measurement capabilities. This was done using a fixture with a built-in linear Vernier Caliper to measure a known distance, which allowed installation of either the S-Track or the IR-TRACC instrumentation. For each instrumentation type, four thoracic and two abdominal sensors were calibrated.

Static Positioning Tests. The THOR-50M 3D IR-TRACC set up fixture was used in conducting this test (
Figure 6). One measurement device (S-Track or IR-TRACC) was selected from the left side at each ATD location (upper thorax, lower thorax, lower abdomen), and the IR-TRACC or the S-Track was installed into the setup fixture.

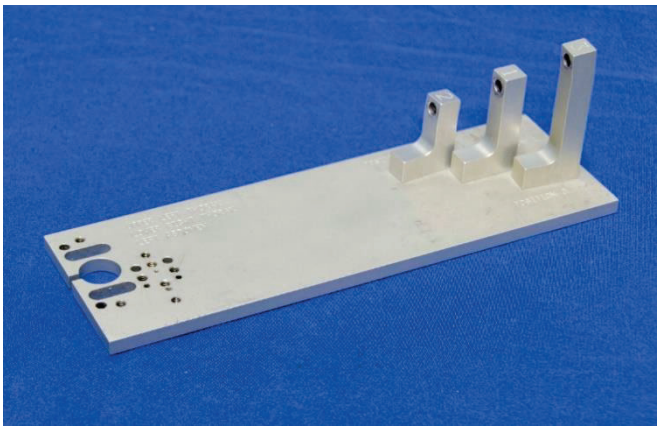

Figure 6: THOR-50M 3D IR-TRACC set up fixture (472-6000)

Since the end of each measurement device has a U-joint which could swivel and lead to increased error during data collection, a Teflon collar was installed over the U-joint of both the IR-TRACC and the S-Track to prevent pivoting (Figure 7). This also provided a distinct point for the FARO measurement at the end of the U-joint.

To conduct the static tests, the end of the IR-TRACC or S-Track was moved to various random angles and lengths as illustrated in Figure 7. At each position, a 3D FARO point (X, Y, Z) location was collected. Simultaneously, the data acquisition system collected the data from the rotary potentiometers and IR-TRACC or S-Track. Once the data was collected, the electronic data was processed to obtain the X, Y, and Z coordinates calculated from the rotary potentiometers and IR-TRACC or S-Track. This data was then directly compared to the data collected by the FARO. The test matrix for the static comparison tests is given in Table 2.

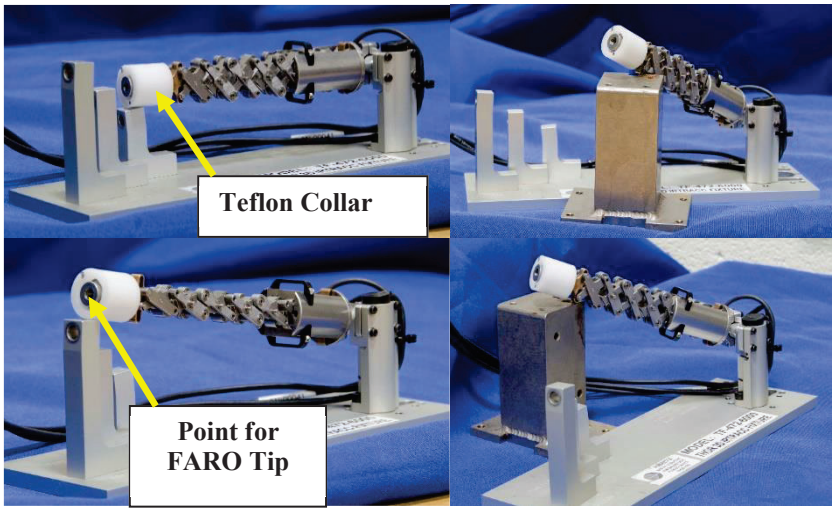

Figure 7: Examples of static test point collection

Table 2. Test Matrix for Static S-Track and IR-TRACC Comparison Study

Purpose	Sensor	Test Type	Full Scale or Component Tests	Test Device	Description	Device Description	Number of Tests
Device Accuracy in IR-TRACC gimbal	IR-TRACC	Static	Component	3D IR-TRACC set up fixture	Use FARO to compare X, Y, Z to calculated IR-TRACC or S-Track outputs	Upper Left Thorax	12 positions varying angles & lengths
						Lower Left Thorax	
	S-Track					Lower Left Abdomen	

Dynamic Tests

Dynamic tests included qualification and sled tests.

*Qualification Tests***.** For qualification testing, IR-TRACC and S-Track sensors were integrated into THOR-50M Serial No. 007. This particular THOR unit is built to the latest specifications (see docket NHTSA-2019-0106). Upper thorax, lower thorax, and abdomen qualification tests were conducted (and passed) (Table 3) using the procedures in the THOR-50M qualification procedures manual (NHTSA, 2018). One series was conducted with the IR-TRACCs installed and the other with the S-Tracks. A qualitative comparison showing overlays of the specified responses is included.

Table 3. Test Matrix for Dynamic Qualification S-Track and IR-TRACC Comparison Study

Purpose	Sensor	Test Type	Full Scale or Component Tests	Test Device	Description	Device Description	Number of Tests
Dynamic Qualification Test Performance Comparison	IR-TRACC	Dynamic Qualification	Full Scale	Installed in THOR-50M SN 007	Upper Thorax	IR-TRACCs in all locations	5
					Lower Thorax Left Side		5
					Lower Abdomen		5
	S-Track				Upper Thorax	S-Tracks in all locations	5
					Lower Thorax Left Side		5
					Lower Abdomen		5

*Sled Tests***.** For sled testing, IR-TRACC and S-Track sensors were integrated into THOR-50M Serial No. DL9207. This particular THOR unit is built to the latest specifications (see docket NHTSA-2019-0106). Sled tests were performed with the THOR-50M in two conditions: one with the IR-TRACC in all locations,

and one with the S-Track in all locations (Table 4). The objective of these sled tests was threefold: 1.) to assess whether the measurement ability of the IR-TRACC and S-Track are equivalent, 2.) to examine the durability of the S-Track in a vehicle crash environment, and 3.) to examine whether the S-Track exhibited the same noise artifacts seen in the IR-TRACC in vehicle crash environments.

Table 4. Sled Test Matrix

Purpose	Sensor	Test Type	Full Scale or Component Tests	Test Device	Description	Device Description	# of Tests
Dynamic Performance	IR-TRACC	Dynamic Sled	Full Scale	Installed in THOR-50M SN DL9207	Near-side Frontal Oblique Crash Sled Simulation	IR-TRACCs in all locations	2
	S-Track (rotated)*				Near-side Frontal Oblique Crash Sled Simulation	S-Tracks in all locations	4

*See *Sled Tests* section.

The sled test environment consisted of a rigidized buck representative of the front half of a mid-sized passenger vehicle, rotated 20° to simulate a near-side frontal oblique crash. The crash pulse was configured to reproduce the resultant vehicle acceleration and change in velocity of a frontal oblique crash test of the same vehicle, a Chevrolet Malibu (NHTSA TSTNO v09476). Production seats and restraints, including the seat belt, frontal airbag, and side curtain airbag, were installed and triggered to match their deployment time in the associated crash test. The THOR-50M was seated in the driver's seat and positioned using the prescribed seating procedures (Louden, 2019).

RESULTS

Static Tests

Installation. NHTSA specified that the S-Track sensors must match (at least) the connected, extended, effective peak deflection, and effective deflection range dimensions of the IR-TRACCs on the THOR-50M drawings. The thorax S-Track sensors' fully extended distance of 152.1 mm and fully collapsed distance of 56.1 mm (delta = 96 mm) exceeded the requirement to measure 90 mm of deflection within the THOR-50M thorax (Figure 8**Error! Reference source not found.**).

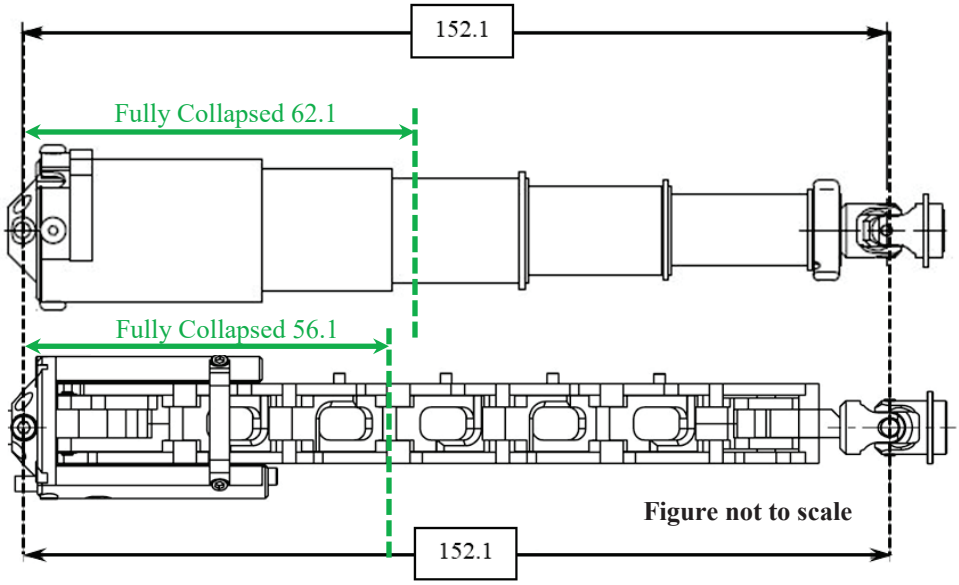

Figure 8: IR-TRACC (top) and S-Track (bottom) fully extended and collapsed lengths for thorax

The rationale used to determine the deflection range requirements for replacement abdominal sensors is different than the rationale used to determine the deflection range requirements for replacement thoracic sensors. In the thorax, the total deflection of the sensors is limited only by the fully collapsed length of the device, making it essential for replacement sensors to provide at least the same fully collapsed length as the IR-TRACCs. However, the design of the abdomen itself, *not the fully collapsed length of the device*, is what limits the total deflection of the abdominal sensors. The abdomen's design integrates the use of an overload cone to prevent the sensor from completely collapsing during compression (indicated with the dashed red line in Figure 9). By design, the anterior attachment point of the deflection sensor must be able to collapse further than the location of the overload cone, thus ensuring that the maximum deflection that can be achieved in the abdomen (anterior attachment point to the overload cone) is measured by the sensor. The overload cone is 89.5 mm from the sensor's posterior attachment point. Since the S-track fully collapses to 72.6 mm from the posterior attachment point, it meets the requirement of being able to collapse beyond the overload cone (Figure 9).

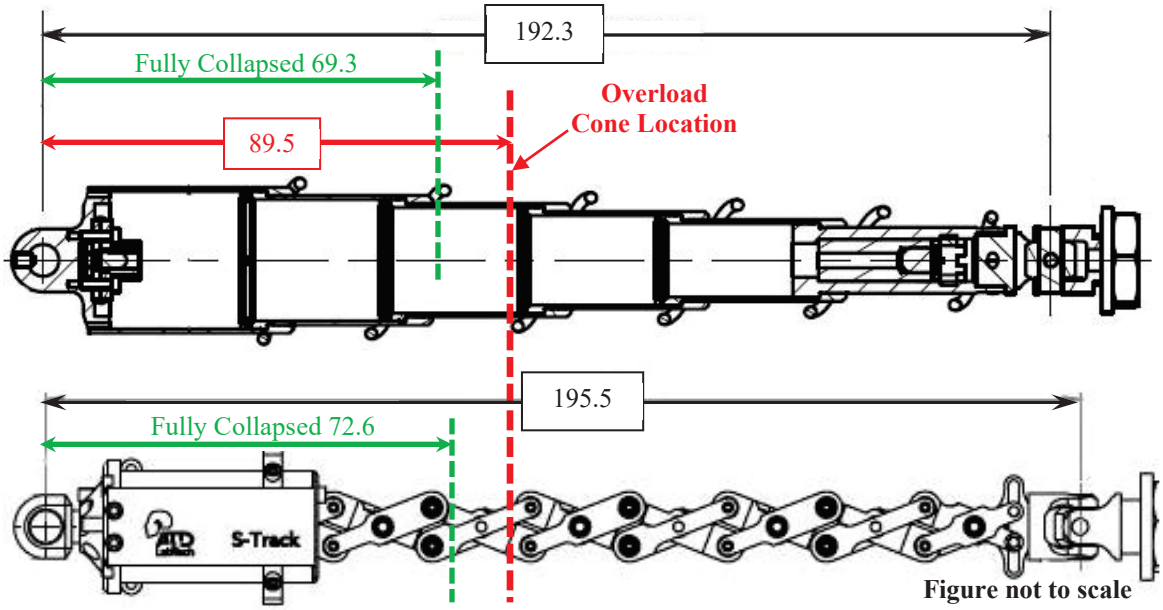

Figure 9: IR-TRACC (top) and S-Track (bottom) fully extended and collapsed lengths for abdomen

Calibration. The thoracic and abdominal deflection sensors were calibrated to ensure proper measurement capabilities. The results confirmed that the range of measurement of the S-Track was consistent with the range of measurement of the IR-TRACC, and all sensors met their respective manufacturer's specification for the maximum allowable linear error as a percentage of full scale (Table 5**Error! Reference source not found.**). While both abdominal instruments are capable of measuring slightly more than 120 mm of deflection, both were calibrated to 120 mm for consistency.

Table 5. Calibration of IR-TRACC and S-Track Sensors

	IR-TRACC		S-Track	
Sensor Location	**Range [mm]**	**Linear Error (% of Full Scale) [≤ 2%]**	**Range [mm]**	**Linear Error (% of Full Scale) [≤ 0.5%]**
Upper Left Thorax	90	0.08	90	0.28
Upper Right Thorax	90	0.12	90	0.10
Lower Left Thorax	90	0.09	90	0.11
Lower Right Thorax	90	0.19	90	0.38
Left Abdomen	120	0.33	120	0.32
Right Abdomen	120	1.47	120	0.27

Static Positioning Tests. Table 6 through Table 9 provides the static positioning comparison data between the S-Track and FARO or IR-TRACC and FARO measurement for the upper left thorax assembly. This exercise was performed for all S-Tracks and IR-TRACCs in the study, but only the detailed information for the upper left thorax sensors are shown to provide a representative example. The FARO points were compared to the S-Track and IR-TRACC measurements and the absolute difference was calculated.

Table 6. Upper Left Thorax X Static Test Results S-Track and IR-TRACC

Upper Left Thorax				
Instrumentation	**Point**	**FARO X (mm)**	**S-Track or IR-TRACC X (mm)**	**Absolute Difference X (mm)**
S-Track	S-Track Pt1	157.31	157.77	0.46
	S-Track Pt2	177.71	178.19	0.48
	S-Track Pt3	151.67	152.04	0.37
	S-Track Pt4	138.05	138.72	0.67
	S-Track Pt5	166.34	167.45	1.12
	S-Track Pt6	114.21	114.94	0.73
	S-Track Pt7	112.55	113.03	0.48
	S-Track Pt8	104.04	104.99	0.95
	S-Track Pt9	136.21	136.96	0.75
	S-Track Pt10	110.28	110.05	0.22
	S-Track Pt11	83.77	84.30	0.53
	S-Track Pt12	117.03	117.56	0.53
Average Difference				**0.61**
Standard Deviation of Difference				**0.25**
IR-TRACC	IR-TRACC Pt 1	163.45	165.60	2.15
	IR-TRACC Pt 2	177.39	179.57	2.18
	IR-TRACC Pt 3	147.20	151.48	4.29
	IR-TRACC Pt 4	168.55	169.40	0.84
	IR-TRACC Pt 5	124.36	124.31	0.05
	IR-TRACC Pt 6	98.70	102.02	3.32
	IR-TRACC Pt 7	107.89	110.44	2.55
	IR-TRACC Pt 8	96.40	96.33	0.06
	IR-TRACC Pt 9	141.31	145.21	3.91
	IR-TRACC Pt 10	67.60	69.19	1.59
	IR-TRACC Pt 11	78.76	81.89	3.13
	IR-TRACC Pt 12	142.43	143.85	1.43
Average Difference				**2.13**
Standard Deviation of Difference				**1.40**

Table 7. Upper Left Thorax Y Static Test Results for S-Track and IR-TRACC

Upper Left Thorax				
Instrumentation	**Point**	**FARO Y (mm)**	**S-Track or IR-TRACC Y (mm)**	**Absolute Difference Y (mm)**
S-Track	S-Track Pt1	-2.87	-3.77	0.90
	S-Track Pt2	-16.91	-18.07	1.16
	S-Track Pt3	0.30	-0.05	0.34
	S-Track Pt4	19.04	19.14	0.10
	S-Track Pt5	-10.59	-11.36	0.77
	S-Track Pt6	1.71	1.68	0.03
	S-Track Pt7	1.57	1.17	0.40
	S-Track Pt8	23.17	22.95	0.23
	S-Track Pt9	-71.37	-72.06	0.69
	S-Track Pt10	-52.82	-53.22	0.40
	S-Track Pt11	6.02	5.85	0.17
	S-Track Pt12	5.27	5.45	0.18
Average Difference				**0.45**
Standard Deviation of Difference				**0.35**
IR-TRACC	IR-TRACC Pt 1	0.70	-1.87	2.57
	IR-TRACC Pt 2	-15.91	-18.77	2.87
	IR-TRACC Pt 3	-9.13	-10.49	1.37
	IR-TRACC Pt 4	15.60	13.53	2.06
	IR-TRACC Pt 5	21.01	18.89	2.12
	IR-TRACC Pt 6	24.07	23.70	0.37
	IR-TRACC Pt 7	-29.03	-30.63	1.61
	IR-TRACC Pt 8	-50.05	-53.89	3.84
	IR-TRACC Pt 9	-48.53	-49.95	1.42
	IR-TRACC Pt 10	33.23	33.01	0.21
	IR-TRACC Pt 11	33.16	33.75	0.60
	IR-TRACC Pt 12	-68.73	-71.71	2.98
Average Difference				**1.83**
Standard Deviation of Difference				**1.12**

Table 8. Upper Left Thorax Z Static Test Results for S-Track and IR-TRACC

Upper Left Thorax				
Instrumentation	**Point**	**FARO Z (mm)**	**S-Track or IR-TRACC Z (mm)**	**Absolute Difference Z (mm)**
S-Track	S-Track Pt1	25.11	25.41	0.30
	S-Track Pt2	9.50	7.73	1.77
	S-Track Pt3	94.14	94.93	0.80
	S-Track Pt4	-19.60	-18.82	0.78
	S-Track Pt5	-60.67	-59.87	0.80
	S-Track Pt6	-13.04	-12.47	0.57
	S-Track Pt7	41.82	42.14	0.32
	S-Track Pt8	-50.50	-50.44	0.06
	S-Track Pt9	-9.78	-8.20	1.58
	S-Track Pt10	77.44	79.16	1.72
	S-Track Pt11	-6.00	-5.65	0.34
	S-Track Pt12	-1.62	-0.90	0.72
Average Difference				**0.81**
Standard Deviation of Difference				**0.58**
IR-TRACC	IR-TRACC Pt 1	29.75	34.42	4.67
	IR-TRACC Pt 2	13.61	16.90	3.29
	IR-TRACC Pt 3	-55.22	-52.42	2.80
	IR-TRACC Pt 4	56.60	62.18	5.58
	IR-TRACC Pt 5	84.47	90.29	5.82
	IR-TRACC Pt 6	-49.71	-48.47	1.24
	IR-TRACC Pt 7	-16.11	-14.37	1.74
	IR-TRACC Pt 8	74.00	76.87	2.87
	IR-TRACC Pt 9	-84.79	-83.73	1.06
	IR-TRACC Pt 10	42.09	46.30	4.21
	IR-TRACC Pt 11	-15.16	-13.75	1.40
	IR-TRACC Pt 12	-11.29	-8.66	2.63
Average Difference				**3.11**
Standard Deviation of Difference				**1.65**

Table 9. Upper Left Thorax Resultant Static Test Results for S-Track and IR-TRACC

Upper Left Thorax				
Instrumentation	**Point**	**FARO Resultant (mm)**	**S-Track or IR-TRACC Resultant (mm)**	**Absolute Difference Resultant (mm)**
S-Track	S-Track Pt1	159.32	159.85	0.53
	S-Track Pt2	178.76	179.27	0.50
	S-Track Pt3	178.51	179.24	0.73
	S-Track Pt4	140.73	141.29	0.56
	S-Track Pt5	177.37	178.19	0.82
	S-Track Pt6	114.96	115.63	0.66
	S-Track Pt7	120.08	120.64	0.56
	S-Track Pt8	117.95	118.72	0.77
	S-Track Pt9	154.08	154.98	0.89
	S-Track Pt10	144.73	145.64	0.90
	S-Track Pt11	84.20	84.69	0.49
	S-Track Pt12	117.16	117.69	0.53
Average Difference				**0.66**
Standard Deviation of Difference				**0.16**
IR-TRACC	IR-TRACC Pt 1	166.13	169.15	3.01
	IR-TRACC Pt 2	178.62	181.34	2.72
	IR-TRACC Pt 3	157.48	160.64	3.16
	IR-TRACC Pt 4	178.48	180.95	2.47
	IR-TRACC Pt 5	151.80	154.80	3.00
	IR-TRACC Pt 6	113.10	115.40	2.30
	IR-TRACC Pt 7	112.88	115.51	2.62
	IR-TRACC Pt 8	131.43	134.51	3.08
	IR-TRACC Pt 9	171.79	174.91	3.12
	IR-TRACC Pt 10	86.28	89.56	3.28
	IR-TRACC Pt 11	86.79	89.63	2.85
	IR-TRACC Pt 12	158.55	160.97	2.42
Average Difference				**2.84**
Standard Deviation of Difference				**0.32**

Table 10 summarizes the results of all static positioning tests. The table displays the average differences between the FARO measurements and the S-Track or IR-TRACC. The S-Track average differences range from 0.45 mm to 2.19 mm with eight of the 12 averages at or below 1.00 mm (green shading in Table 10). The IR-TRACC differences range from 0.62 mm to 3.11 mm with two of the 12 averages at or below 1.00 mm. Standard deviations for both devices were below 2.0 mm. Results indicate that the S-Track can measure at least as well as, or better than, the IR-TRACC in a static environment.

Table 10. Comparison of Average Differences Between S-Track and IR-TRACC in Static Tests

Test Assembly	Device	AVG. Absolute Difference X (mm)	AVG. Absolute Difference Y (mm)	AVG. Absolute Difference Z (mm)	AVG. Absolute Difference Resultant (mm)
Upper Left Thorax Assembly	S-Track	0.61	0.45	0.81	0.66
	IR-TRACC	2.13	1.83	3.11	2.84
Lower Left Thorax Assembly	S-Track	1.00	2.19	1.29	1.28
	IR-TRACC	1.36	2.20	1.83	1.44
Lower Left Abdomen Assembly	S-Track	0.69	0.99	1.27	0.60
	IR-TRACC	1.26	0.62	0.74	1.16

***green shading indicates differences ≤ 1.00 mm**

Dynamic Tests

Qualification Tests. Figure 10 through Figure 12 provide the comparison data between the S-Track and IR-TRACC measurements for the upper left thorax assembly. Only plots for X-axis deflection, Z-axis deflection, and resultant deflection are presented because the Y-axis deflections were all below 5 mm.

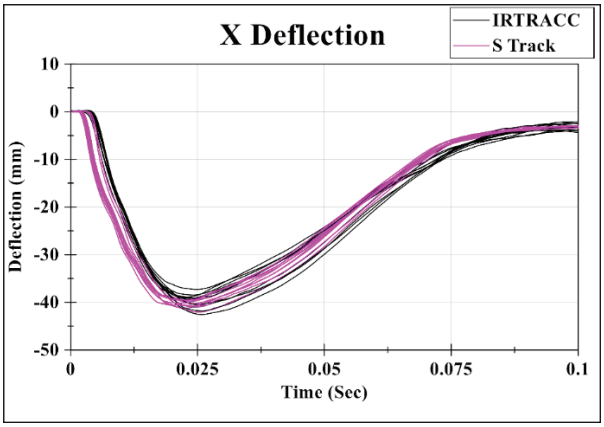

Figure 10: IR-TRACC and S-Track left and right X-axis deflections for upper thorax qualification tests

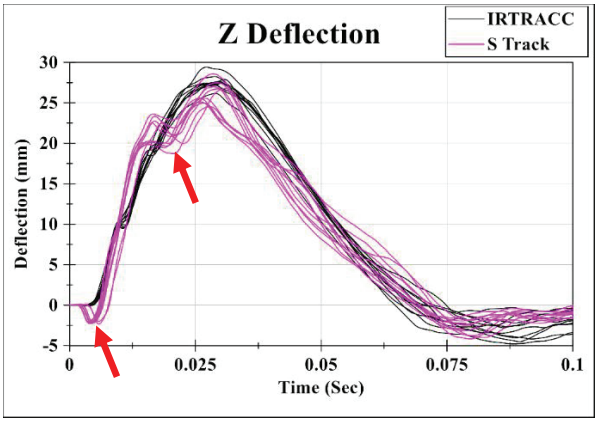

Figure 11: IR-TRACC and S-Track left and right Z-axis deflections for upper thorax qualification tests

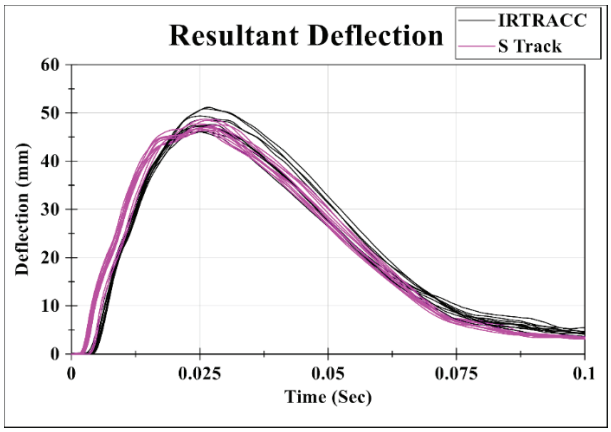

Figure 12: IR-TRACC and S-Track left and right resultant-deflections for upper thorax qualification tests

In all cases but one, the deflection time-histories of the S-Track and IR-TRACC tests demonstrate similar shapes and magnitutes. In the upper thorax tests using the S-Track, some inflection point anomalies in the Z-axis deflection time-history are evident (see red arrows in Figure 11). These inflections are not present in the IR-TRACC data. Furthermore, they are present on both the left and right side Z-axis deflections in the S-Track tests indicating that the cause is not likely an isolated instrument malfunction.

Further investigation using the raw data from the IR-TRACC and S-Track deflections and the Y and Z potentiometers showed that the Y-axis potentiometer data (Figure 13) revealed inflections which mimicked those found in the S-Track Z-axis deflection data. Again, these anomalies were not present in the Y-axis potentiometer on the IR-TRACC tests. The S-track and IR-TRACC raw deflections do not have inflections, so the data collected from the instruments themselves does not appear to be the direct source of the anomalies.

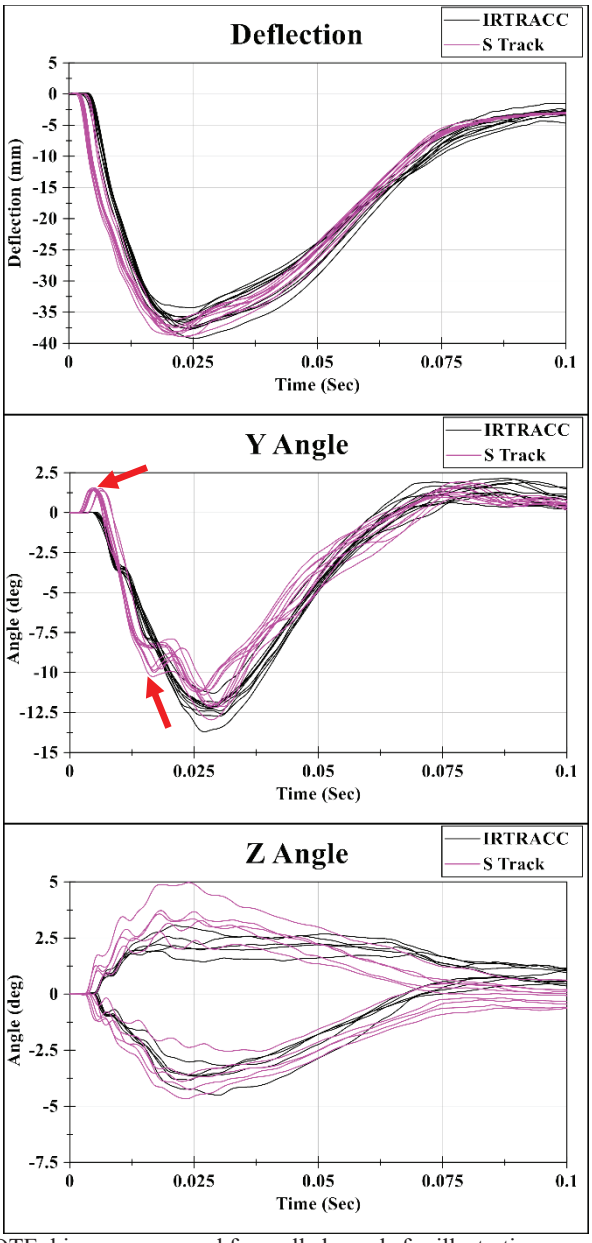

*NOTE: bias was removed from all channels for illustrative purposes

Figure 13. IR-TRACC and S-Track raw signals for upper thorax tests

One possible cause of the inflections could be the U-joint at the anterior end of the S-track. The S-Track manufacturer supplied this part, and it differs from the U-joints used with the IR-TRACC (Figure **14**); this may cause differences in the performance. S-Track installation into the ATD followed procedures in the PADI for orientation of the U-joints, but these instructions were written for the IR-TRACC U-joint design; there may be differences between the two U-joints where this procedure does not apply to the S-track joint (NHTSA, 2020).

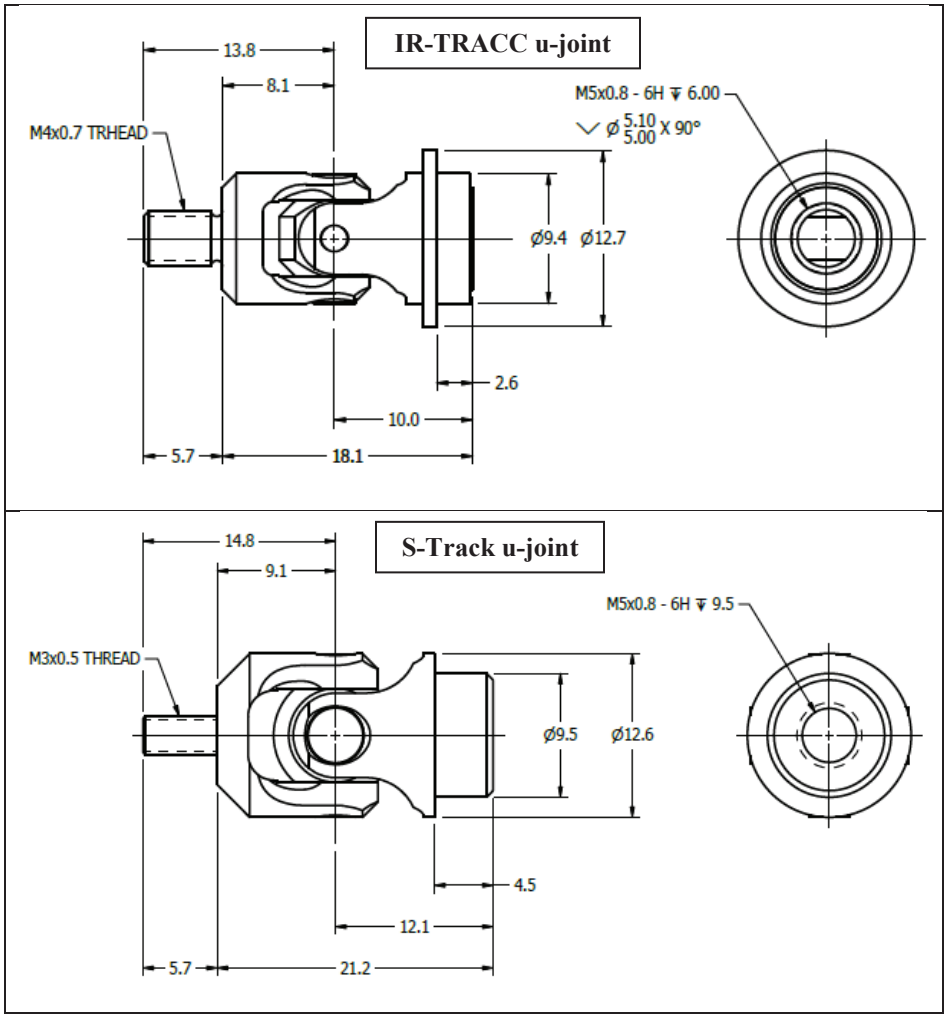

Figure 14. Comparison of IR-TRACC u-joint and S-Track u-joint dimensions

Another theory for the inflections includes the scissor mechanisms of the S-track bouncing the Y-axis potentiometer. Note that the Z-axis potentiometer, although small in magnitude, does also appear to "bounce". The effects of off-axis loading on the deflection measurement is currently measured by the manufacturer for IR-TRACCs prior to sale, but the effects of this loading were not measured for the S-Tracks (or IR-TRACCs) in this study. However, qualitatively, the design of S-Track appears to allow more flexion when an off-axis force is applied to the center compared to the IR-TRACC. This lends to the theory that flexing of the S-track may cause the inflections which are seen in the potentiometers.

The tabulated results presented in Table 11 examine the peak upper thorax qualification test responses. These tests all passed the current qualification specifications except for the cells highlighted in yellow, which are outside of the current 2409 – 2944 N qualification requirements. At the time of testing (2017), these values were considered passing, but the corridors were adjusted in 2018, resulting in values outside of the specifications. The coefficient of variation (CV) is the ratio of the standard deviation to the mean (CV = SD/mean); lower CVs indicate better repeatability between measured values. In this table, the CVs are better for the S-Track compared to the IR-TRACC for all the measurements evaluated. Based on CVs, the S-Track measurements were more repeatable than the IR-TRACC measurements for this test mode.

Table 11. Upper Thorax Dynamic Qualification Repeatability

Sensor		Test No.	Overall Peak Force (N)	Peak Upper Left XYZ Resultant Deflection (mm)	Peak Upper Right XYZ Resultant Deflection (mm)	Force at Max Left Resultant Deflection (N)	Force at Max Right Resultant Deflection (N)
S-Track		171113-5	2837	50.0	46.7	2318	2409
		171113-6	2872	46.9	47.8	2355	2439
		171113-8	2754	46.4	46.6	2404	2442
		171113-9	2649	48.7	47.5	2595	2575
		171114-1	2730	47.5	48.4	2395	2547
IR-TRACC		171101-1	2915	47.6	46.0	2318	2480
		171101-2	2706	51.2	47.3	2323	2334
		171101-3	2591	50.8	47.2	2315	2329
		171101-4	2790	49.4	47.3	2562	2533
		171102-1	2693	48.7	46.1	2365	2376
Repeatability S-Track	Average		2768	47.9	47.4	2413	2482
	Std. Dev.		89	1.4	0.8	107	74
	CV %		3.2%	3.0%	1.6%	4.4%	3.0%
Repeatability IR-TRACC	Average		2718	49.2	47.3	2389	2453
	Std. Dev.		123	1.8	0.8	120	116
	CV %		4.5%	3.6%	1.8%	5.0%	4.7%

Figure 15 through Figure 18 provide the comparison data between the S-Track and IR-TRACC measurements for the lower left thorax assembly. Plots for X-axis deflection, Y-axis deflection, Z-axis deflection, and resultant deflection are presented.

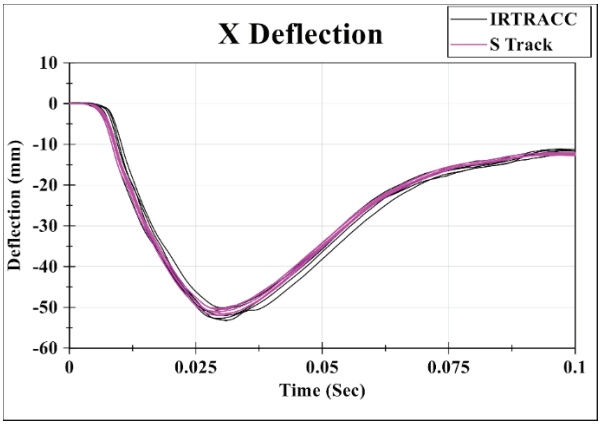

Figure 15: IR-TRACC and S-Track X-axis deflections for left lower thorax qualification tests

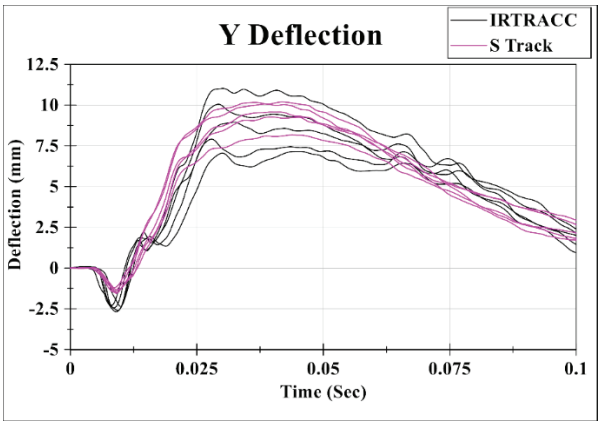

Figure 16: IR-TRACC and S-Track Y-axis deflections for left lower thorax qualification tests

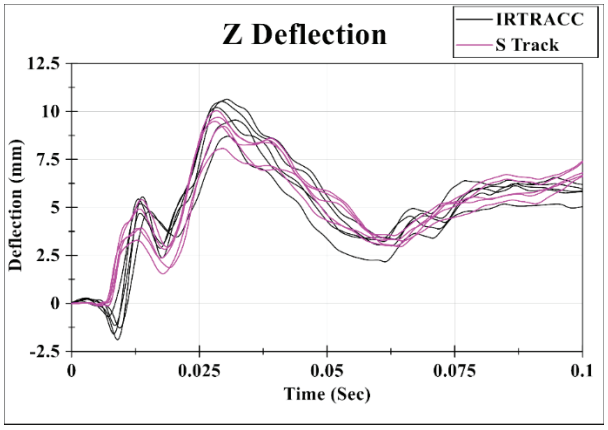

Figure 17: IR-TRACC and S-Track Z-axis deflections for left lower thorax qualification tests

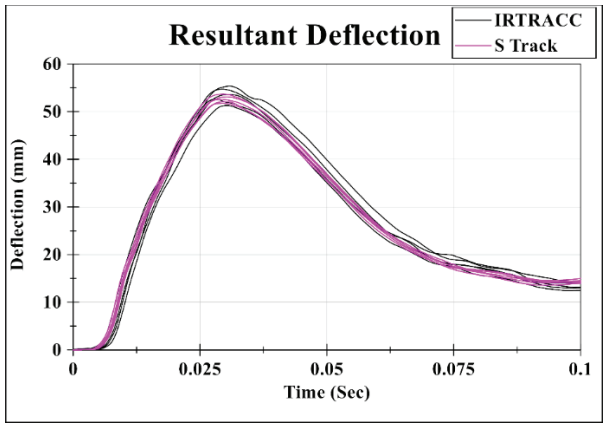

Figure 18: IR-TRACC and S-Track resultant-deflections for left lower thorax qualification tests

The tabulated results presented in Table 12 examine the peak lower thorax responses. These tests all passed the current qualification specifications. Based on CVs, which are lower for the S-Track than the IR-TRACC, the S-Track measurements were more repeatable than the IR-TRACC for this test mode.

Table 12. Lower Thorax Dynamic Qualification Repeatability

Sensor		Test No.	Peak Force (N)	Left or Right Resultant Max Deflection at Peak Force (mm)
S-Track		171109-3	3261	50.7
		171109-6	3268	52.4
		171109-8	3263	51.4
		171109-9	3278	53.4
		171113-1	3292	51.1
IR-TRACC		171102-5	3156	50.5
		171102-7	3380	49.8
		171102-10	3291	52.8
		171106-1	3309	54.5
		171106-2	3317	51.9
Repeatability S-Track	Average		3272	51.8
	Std. Dev.		13	1.1
	CV %		0.4%	2.1%
Repeatability IR-TRACC	Average		3279	51.5
	Std. Dev.		80	1.5
	CV %		2.4%	2.9%

Figure 19 provides the comparison data between the S-Track and IR-TRACC measurements for the lower abdomen assembly. Only the plot for X-axis deflection is presented since the Y-axis and Z-axis measurements were less than about 15 mm and 5 mm, respectively. The results in Figure 19 show similar magnitudes between the S-Track and IR-TRACC measurements.

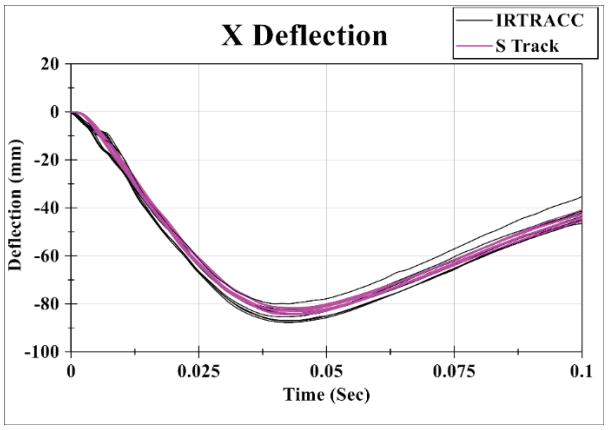

Figure 19: IR-TRACC and S-Track left and right X-axis deflections for lower abdomen qualification tests

The tabulated results presented in Table 13 examine the peak lower abdomen responses. These tests all passed the current qualification specifications. Based on CV, the S-Track measurements were at least as repeatable as the IR-TRACC measurements for this test mode.

Table 13. Lower Abdomen Dynamic Qualification Repeatability

Sensor		Test No.	Overall Peak Force (N)	Left X Deflection at Peak Force (mm)	Right X Deflection at Peak Force (mm)	Difference Peak X Deflection (mm)
S-Track		171108-4	2731	-81.3	-82.7	1.3
		171108-6	2858	-81.8	-83.3	1.4
		171108-8	2803	-79.9	-82.5	2.4
		171108-11	2903	-81.1	-83.8	2.5
		171109-1	2796	-79.9	-81.4	1.5
IR-TRACC		171106-7	2857	-81.1	-79.1	2.5
		171107-1	2810	-82.7	-86.3	2.9
		171107-2	2753	-81.8	-84.5	2.3
		171107-4	2797	-83.4	-86.3	2.7
		171107-7	2808	-82.8	-86.6	3.6
Repeatability S-Track	Average		2818	-80.8	-82.7	1.8
	Std. Dev.		65	0.9	0.9	0.6
	CV %		2.3%	1.1%	1.1%	N/A
Repeatability IR-TRACC	Average		2824	-81.3	-83.0	2.3
	Std. Dev.		58	1.1	2.8	0.5
	CV %		2.0%	1.3%	3.4%	N/A

*Sled Tests***.** For sled tests, in an attempt to identify the source of the inflections (Figure 11), the S-Tracks were rotated about the X-axis from their original orientations (per the manufacturer's recommendation), resulting in the hinges being oriented along the ATD's Y-axis (Figure 20, Figure 21); this orientation is referred to as the "rotated" configuration throughout this report. Note that qualification tests presented above were conducted in the original orientation (Figure 20).

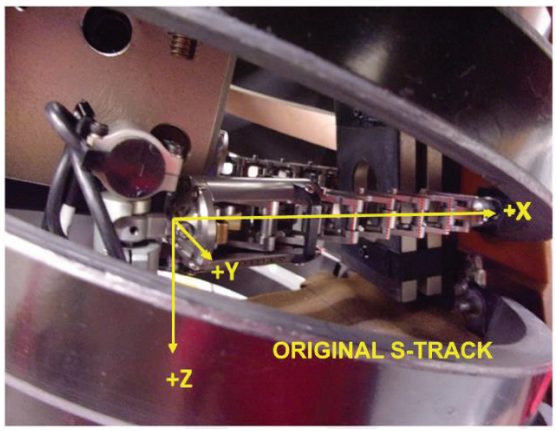

Figure 20: S-Track installed in THOR-50M upper right thorax in original orientation

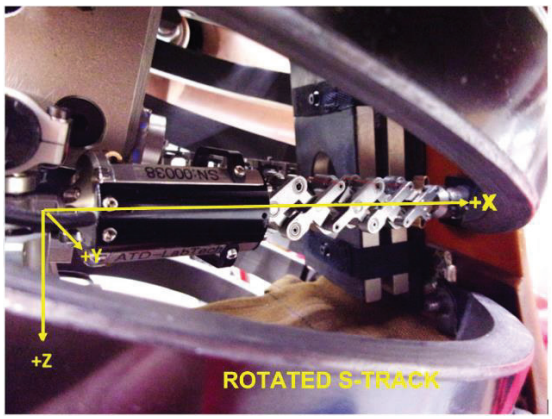

Figure 21: S-Track installed in THOR-50M upper right thorax in rotated orientation

Time-history overlays of the left and right upper thorax deflections, collected during sled testing, can be found in Figure 22 and Figure 23. All angle potentiometers, IR-TRACCs and S-Tracks were filtered to CFC180 (Craig, et al. (2020)). Visually, the upper thorax deflections have similar time-history shapes and magnitudes between the THOR-50M equipped with either IR-TRACCs or S-Tracks. Regardless of whether IR-TRACCs or S-Tracks were used, the quadrant where the peak thoracic deflection occurred was consistently measured at the upper right thorax, as this is the measurement location closest to the shoulder belt. The average peak resultant deflection in the IR-TRACC configuration was 45 mm, while the average peak resultant deflection in the S-Track configuration was 46 mm.

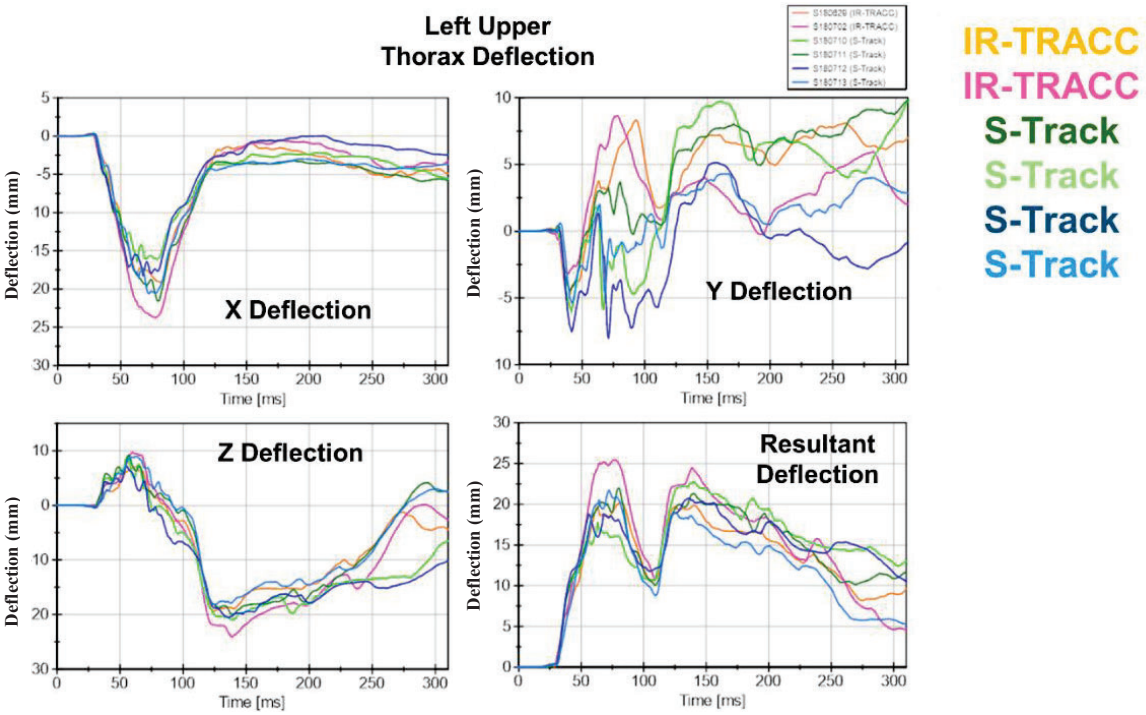

Figure 22: Left upper thorax IR-TRACC and S-Track deflection during sled testing

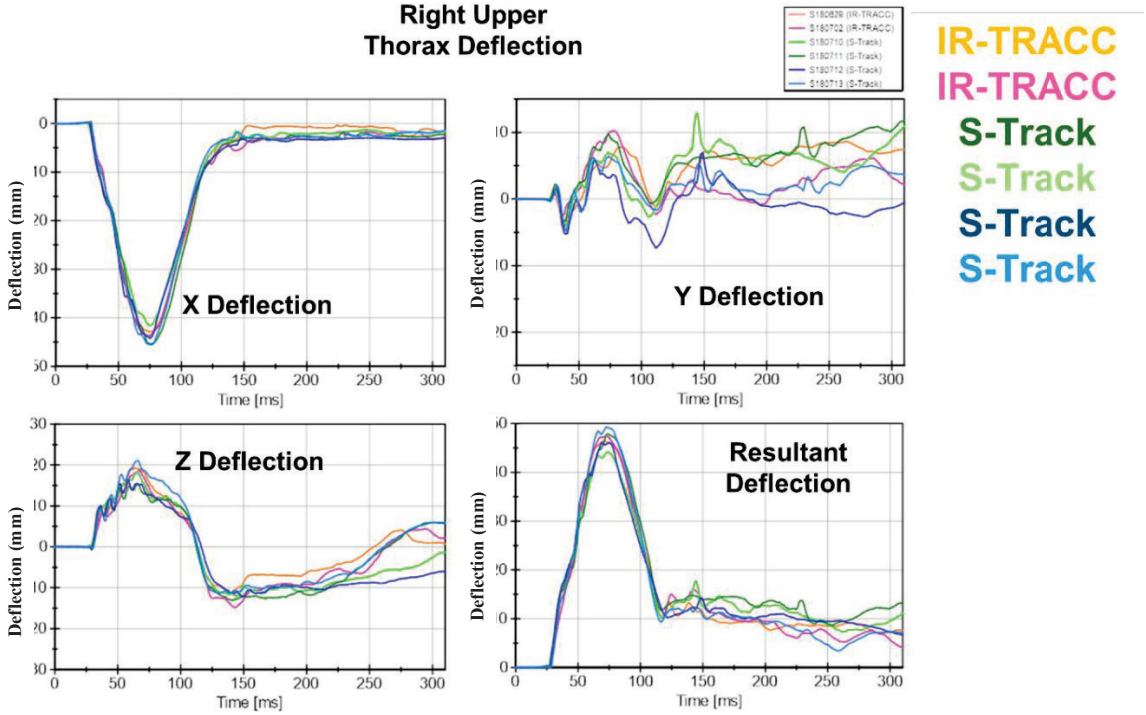

Figure 23: Right upper thorax IR-TRACC and S-Track deflection during sled testing

Left and right lower thorax results from sled testing can be found in Figure 24 and Figure 25, respectively. The lower thorax deflections were also similar between the THOR-50M equipped with either

IR-TRACCs or S-Tracks but IR-TRACC deflections were, for the most part, lower than S-Track deflections. At the left lower thoracic measurement location, which is further away from the belt path, variability in thoracic motion is generally higher. Note that the left lower thorax (Figure 24), shows a positive X deflection, indicating that the deflection point bulges outward, unlike the other three thorax locations.

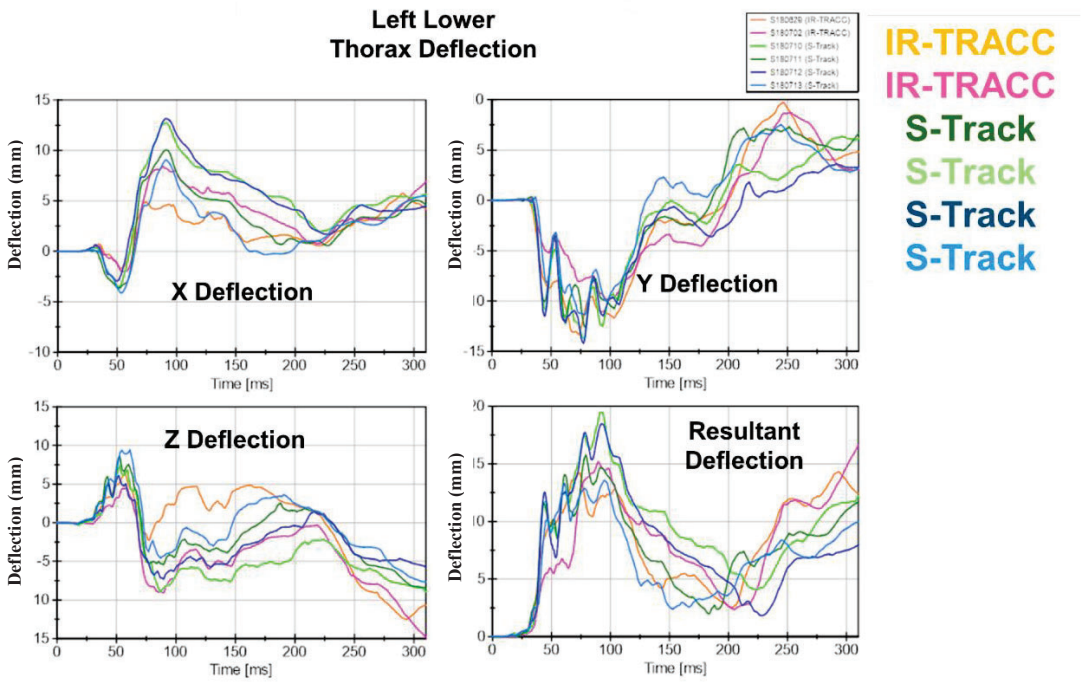

Figure 24: Left lower thorax IR-TRACC and S-track deflection during sled testing

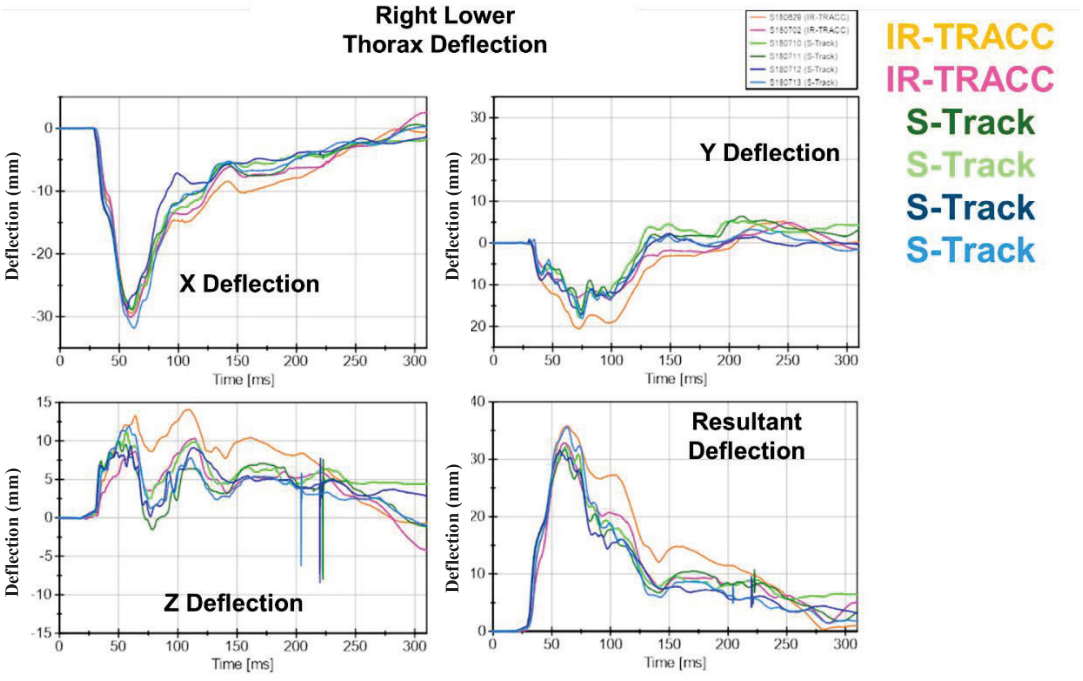

Figure 25: Right lower thorax IR-TRACC and S-Track deflection during sled testing

Left and right lower abdomen results from sled testing can be found in Figure 26 and Figure 27, respectively. At both the right and left abdomen locations, the S-Track recorded deflections that were

consistently lower than the IR-TRACCs, and the average peak deflection measured by the X-axis S-Track was roughly 10 mm lower than that of the IR-TRACC on the right side (Figure 27). However, it is not clear which sensor is more accurate, and whether this variation can be explained by any differences in test setup, belt positioning, or expected test-to-test variation. It is also possible that the S-Track measurement device interacts with the foam inserts of the abdomen under lap belt load, which could stiffen the response. The flat portions on the S-Track Z-axis deflections are likely caused by rotational limitations of the sensor due to contact with the abdomen overload cone and/or abdomen foam; overall the resultant was not affected by the flat spots, and since they occurred late in the event (after 100 ms), this was not investigated further.

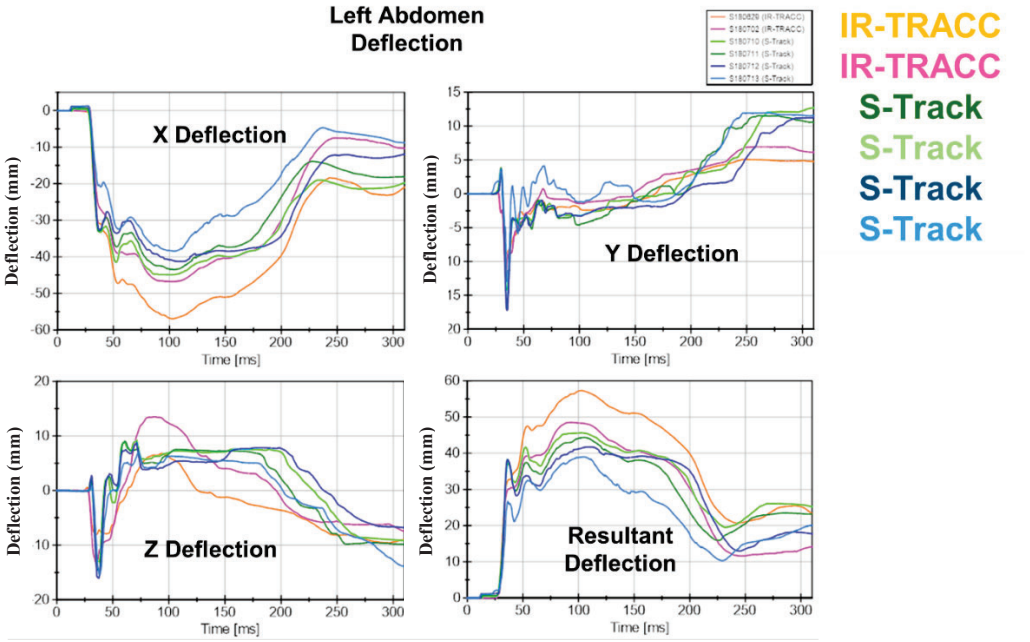

Figure 26: Left abdomen IR-TRACC and S-Track deflection during sled testing

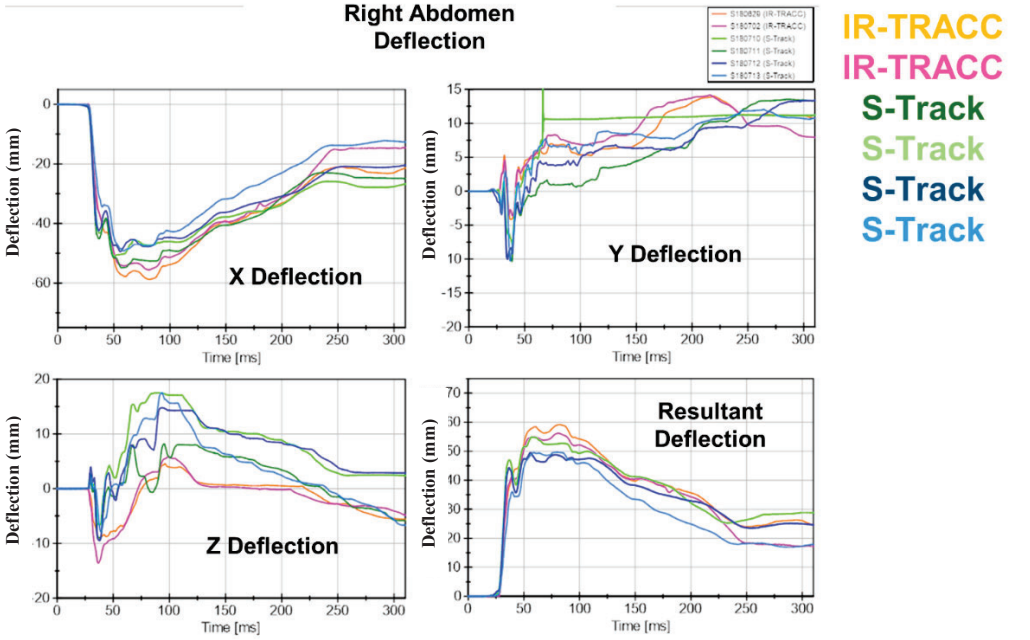

Figure 27: Right abdomen IR-TRACC and S-Track deflection during sled testing

During the sled testing, no damage was found in any of the six S-Tracks and data was successfully collected in all tests. The noise observed in the IR-TRACCs during previous crash and sled testing was also present in the sled tests conducted with the THOR-50M in the IR-TRACC configuration, although to a lesser degree (Figure 28 and Figure 29), and during these tests the noise didn't always occur simultaneously in every IR-TRACC channel as in previous tests (Figure 2); however, the noise was not present in the S-Track configuration (Figure 30). The noise was not thoroughly investigated in this paper, but will be further analyzed in the report (Hagedorn et al., 2021). The S-Track tests did demonstrate some isolated anomalies in the processed deflections, including spikes in the lower right thorax Z-axis deflection (Figure 25, bottom left and right) and flat portions in the right abdomen Y-axis deflection (Figure 27, top right). These anomalies were investigated and determined to result from anomalous potentiometer data channels used to calculate the three-dimensional deflections and not the S-Track channels themselves.

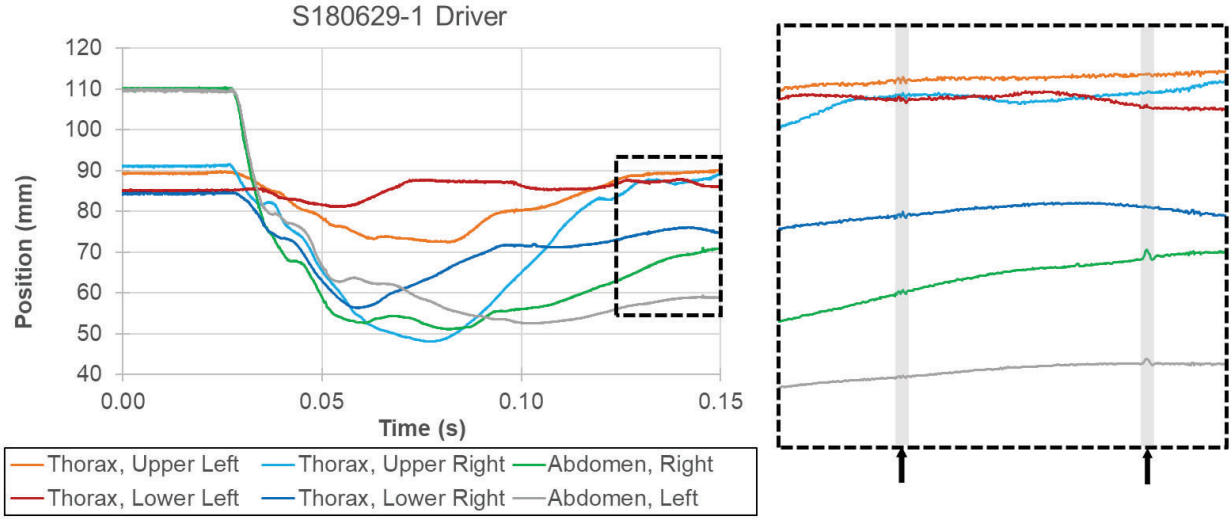

Figure 28: IR-TRACC position time-histories (non-zeroed) from sled test S180629-1

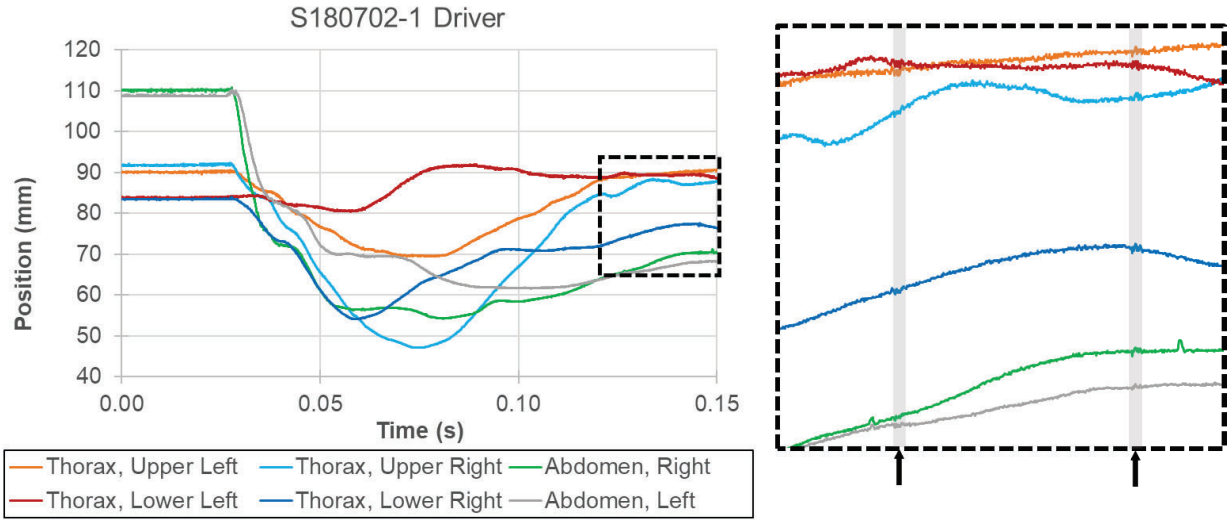

Figure 29: IR-TRACC position time-histories (non-zeroed) from sled test S180702-1

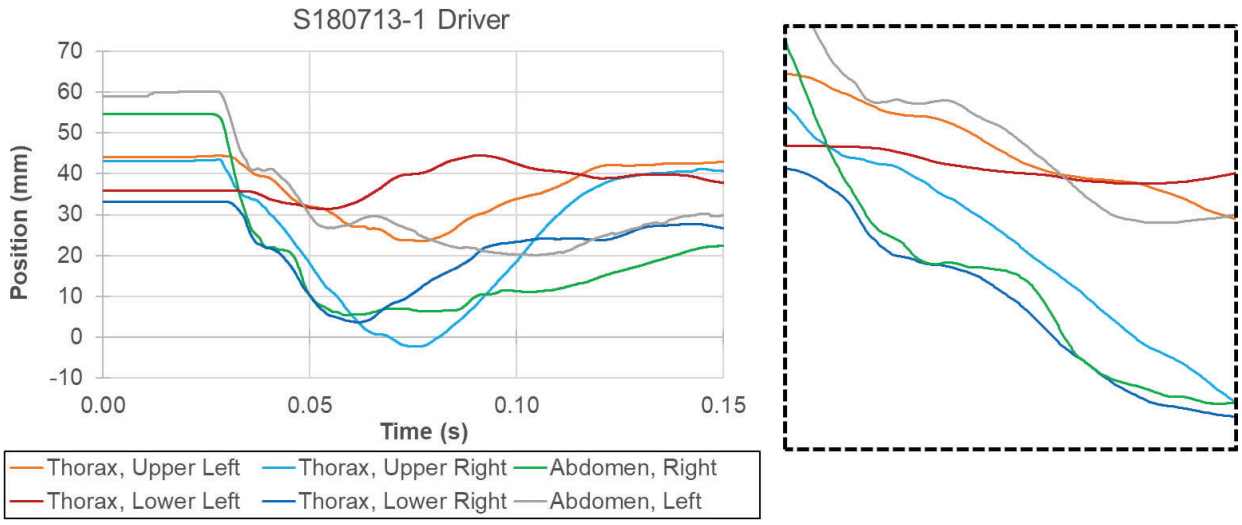

Figure 30: S-Track time-histories (non-zeroed) from sled test S180713-1

Additional "Rotated" S-Track Qualification Tests. Based on the previously conducted upper thorax qualification tests where the S-Track displayed some inflection point anomalies in the Z-axis deflection time-history (Figure 11), only the upper thorax qualification tests were performed after completion of the sled tests. The upper thorax was qualified first with the S-Track in the orientation installed during sled testing ("rotated"), then repeated with the S-Track returned to the "original" position that was used during the previous testing (Figure 20 and Figure 21).

Comparing the upper thorax qualification responses collected from the S-track in the "original" and "rotated" positions, the shapes and the magnitudes of the Z-axis deflection time-histories appear similar, both for the upper left and upper right thorax assemblies (Figure 31). The peak deflections did not appear to be affected by the orientation of the hinges. However, the inflection points of the Z-axis deflection time-histories differ with the hinge orientations both in timing and number of inflection peaks.

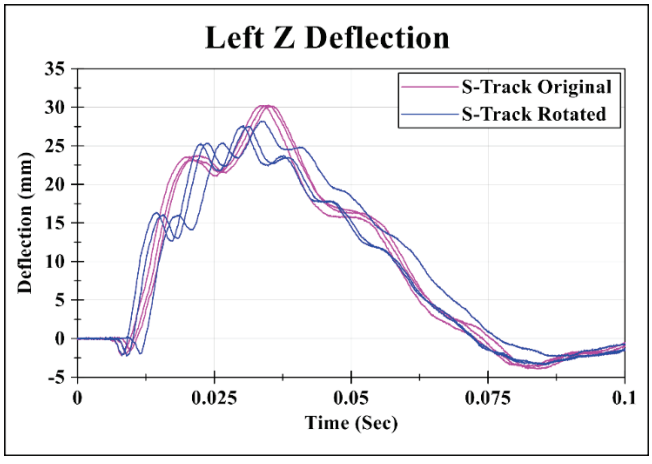

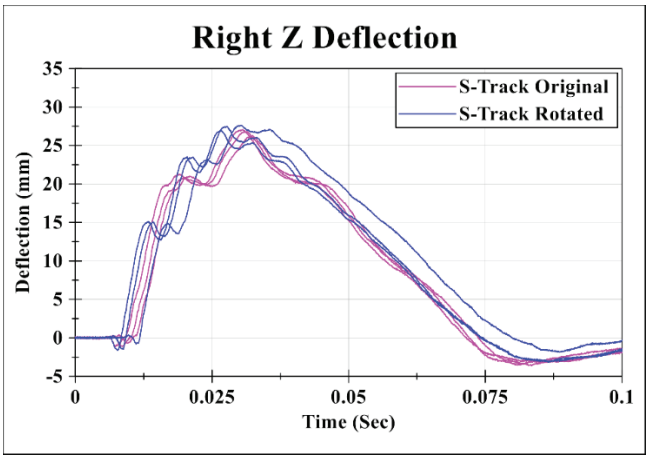

Figure 31: Upper thorax qualification Z deflections in “original” and “rotated” S-Track configurations

CONCLUSIONS

The S-Track integrates into the THOR-50M and meets the desired size, weight, and range of measurement requirements. An examination of the calibration results highlighted that the linearity of the S-Track is comparable or better when compared to the IR-TRACC. Static testing of the S-Track produced measurement deviations from the FARO that were comparable or better than the measurements obtained from the IR-TRACC. The dynamic tests revealed that the repeatability of the S-Track was at least comparable, and often better, then the IR-TRACC. Overall, testing of the S-Track in a variety of scenarios showed that the design is as durable as the IR-TRACC.

While the dynamic peak measurements are mostly equivalent, there are inflections that occur in the upper thorax qualification Z-axis deflection time-histories, regardless of S-Track orientation; these anomalies are not present in the IR-TRACC results. It appears that the measurements recorded by the Y potentiometer contribute significantly to the inflection point, rather than the S-track position output, which has a smooth signal. This is a positive finding since the anomaly is not related to the S-Track motion or electronics. It is believed that the inflection points in the Y potentiometer may be caused by the u-joint design, or the flexibility in the S-Track scissor mechanism, as described below.

Since the S-Track u-joint was a different design than the IR-TRACC u-joint, this may be a possible candidate for future investigations. Furthermore, the design of the S-Track u-joint has changed since these tests were conducted, so the new design could be tested to see if the inflections are still present. Additionally, the S-Track manufacturer, ATD-Labtech, offers an assembly package for the thorax and abdomen which includes the S-Track coupled with two-potentiometers in a gimbal assembly, but that system was not evaluated in this study; future investigation could involve testing the entire assembly made by the manufacturer.

Flexibility in the S-Track could cause the scissor mechanism to “bounce” during compression, and this may contribute to the inflections observed in the potentiometer data. Additional testing with varying loading rate and/or inducing off-axis loading may be useful in determining if the scissor mechanism is bouncing during compression.

Post-test analysis of the dynamic test data indicated that some of the IR-TRACCs contained several low-magnitude noise spikes that occurred at the same time, however, the S-Tracks did not exhibit these same noise spikes during testing. Despite inflections seen in the z-axis deflection, the S-Track appears to offer several improvements over the IR-TRACC in this limited set of tests.

REFERENCES

CRAIG, M., PARENT, D., LEE, E., RUDD, R., TAKHOUNTS, E., & VIKAS H., (2020). Injury Criteria for the THOR50th Male ATD. Washington, DC: National Highway Traffic Safety Administration. Docket NHTSA-2019-0106-0008.

HAGEDORN, A. & MURACH, M. (2021). Evaluation of S-Track as an alternative to the IR-TRACC 3-dimensional deflection measuring device. (Report in process 2021) Washington, DC: National Highway Traffic Safety Administration.

LOUDEN, A.E. (2020, March). Revised THOR 50th percentile male dummy seating procedure. (Report no. DOT HS 812 746). Washington, DC: National Highway Traffic Safety Administration. Docket NHTSA-2019-0106-0006.

NATIONAL HIGHWAY TRAFFIC SAFETY ADMINISTRATION (2018). THOR-50M Drawing Package. Docket No. NHTSA-2019-0106-0002.

NATIONAL HIGHWAY TRAFFIC SAFETY ADMINISTRATION (2018). THOR 50th Percentile Male (THOR-50M) Qualification Procedures Manual, September 2018. Docket NHTSA-2019-0106-0001.

NATIONAL HIGHWAY TRAFFIC SAFETY ADMINISTRATION (2020, March). THOR 50th Percentile Male (THOR-50M) Procedures for Assembly, Disassembly, and Inspection, November 2019. Docket NHTSA-2019-0106-0007.

NCAP comments: https://www.regulations.gov. Docket No. NHTSA-2015-0119.

ROUHANA, S.W., ELHAGEDIAB, A.M., & CHAPP, J.J. (1998). A high-speed sensor for measuring chest deflection in crash test dummies. ESV Conference, 1998, Paper Number 9S-S9-O-15.

SAUNDERS, J. & PARENT D. (2018). Repeatability and reproducibility of oblique moving deformable barrier test procedure. SAE Technical Paper 2018-01-1055. Docket ID NHTSA-2019-0106-0005.

All Authors' full name, address, and e-mail

1. Alena Hagedorn
2. Transportation Research Center Inc.
3. VRTC Building 60, 10820 State Route 347, East Liberty, OH 43319
4. (937) 666-3265
5. alena.hagedorn.ctr@dot.gov

1. Michelle Murach
2. Transportation Research Center Inc.
3. VRTC Building 60, 10820 State Route 347, East Liberty, OH 43319
4. (937) 666-3245
5. michelle.murach.ctr@dot.gov

1. William Millis
2. National Highway Traffic Safety Administration, VRTC
3. VRTC Building 60, 10820 State Route 347, East Liberty, OH 43319
4. (937) 666-3484
5. william.millis@dot.gov

1. Joseph McFadden
2. National Highway Traffic Safety Administration, VRTC (retired)

1. Daniel Parent
2. National Highway Traffic Safety Administration
3. 1200 New Jersey Avenue, S.E., Washington, D.C. 20590
4. (202) 366-1724
5. dan.parent@dot.gov